Doping management for high-power fiber lasers: 100 W, few-picosecond pulse generation from an all-fiber-integrated amplifier

P. Elahi,[1,*] S. Yılmaz,[1] Ö. Akçaalan,[1] H. Kalaycıoğlu,[1] B. Öktem,[2] Ç. Şenel,[1,3] F. Ö. Ilday,[1] and K. Eken[4]

[1]*Department of Physics, Bilkent University, 06800 Ankara, Turkey*

[2]*Institute of Materials Science and Nanotechnology, Bilkent University, 06800 Ankara, Turkey*

[3]*TÜBITAK Ulusal Metroloji Enstitüsü (UME), Gebze, 41470 Kocaeli, Turkey*

[4]*FiberLAST Inc., 06531 Ankara, Turkey*

Corresponding author: pelahi@fen.bilkent.edu.tr

Thermal effects, which limit the average power, can be minimized by using low-doped, longer gain fibers, whereas the presence of nonlinear effects requires use of high-doped, shorter fibers to maximize the peak power. We propose the use of varying doping levels along the gain fiber to circumvent these opposing requirements. By analogy to dispersion management and nonlinearity management, we refer to this scheme as doping management. As a practical first implementation, we report on the development of a fiber laser-amplifier system, the last stage of which has a hybrid gain fiber composed of high-doped and low-doped Yb fibers. The amplifier generates 100 W at 100 MHz with pulse energy of 1 µJ. The seed source is a passively mode-locked fiber oscillator operating in the all-normal-dispersion regime. The amplifier comprises three stages, which are all-fiber-integrated, delivering 13 ps pulses at full power. By optionally placing a grating compressor after the first stage amplifier, chirp of the seed pulses can be controlled, which allows an extra degree of freedom in the interplay between dispersion and self-phase modulation. This way, the laser delivers 4.5 ps pulses with ~200 kW peak power directly from fiber, without using external pulse compression.   © 2012 Optical Society of America

OCIS codes: 060.2320, 140.4050, 320.7090, 140.3510.

There has been much interest in the development of high-power fiber lasers in recent years as a result of the practicality of these lasers, along with the possibility to generate very high powers with excellent beam quality [1–3]. Continuous-wave fiber lasers generate multi-kilowatt powers [1,2], whereas pulses with tens of micro-joules and even few-millijoule energies can be generated in the ultrafast regime using regular [4] and rod-type [5] fibers, respectively. However, there is a well-known trade-off between minimizing thermal effects and non-linear effects, which limit the average and the peak power, respectively.

From an applications point of view, material processing is arguably among the most important applications of fiber lasers, which requires microjoule-level energies at high repetition rates in order to scale up the processing speed. Impressive results have been obtained with rod-type fiber amplifiers [3]. However, these gain media are rigid and rely mostly on free-space beam propagation. Among non-rod-type fiber systems, [6] reports generation of 100 W, 13 ps pulses at 59.8 MHz and [7] reports 100 W, 21 ps pulses at repetition rates of up to 908 MHz, and recently, [8] reports 110 W, ~1 ps pulses at 1.3 GHz.

Here, we propose doping management, in analogy to dispersion management [9] and nonlinearity management [10], to mitigate the trade-off between thermal load and nonlinear effects. In this scheme, the doping level increases along the direction of signal and pump propagation for forward pumping. Initially, signal power is lowest and pump is highest. Starting with low doping ensures that the thermal load is reduced where its impact is greatest. As pump power decreases and signal power increases, doping level increases to minimize the gain length and consequently to minimize the nonlinear effects. Since fibers with continuously varying doping concentrations are not presently available, we utilize two segments of fiber with different doping levels spliced together. The laser system we constructed generates 4.5 ps (with prechirping) and 13 ps (without prechirping), 100 W, 100 MHz pulses from a misalignment-free, all-fiber-integrated amplifier.

We focus on forward pumping, which has two advantages over backward pumping at high powers: Thermal load is lower since signal and pump powers are maximized at opposite ends of the fiber. Even though the B integral is reduced over the gain fiber, this is more than offset by propagation in undoped fibers required for pump delivery in an all-fiber system. Propagation in passive fiber is more detrimental than in gain fiber, since gain filtering limits spectral broadening due to self-phase modulation (SPM), and a fraction of energy transferred to the Stokes wavelength is reduced when laser gain is comparable to Raman gain.

A schematic of the experimental setup is shown in Fig. 1. An in-line amplifier is seeded by a mode-locked
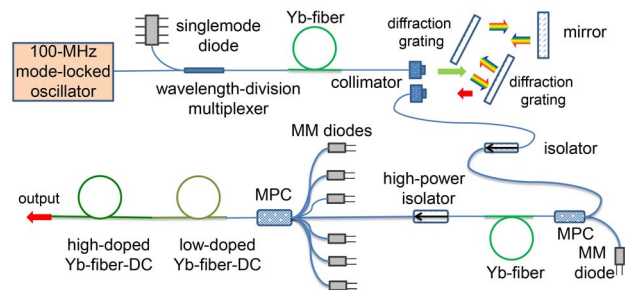

Fig. 1.   (Color online) Schematic of the setup. MM, multimode.

Yb-fiber oscillator, similar in architecture to [11,12]. The seed oscillator operates in the all-normal dispersion (ANDi) regime [13,14] with a repetition rate of 100 MHz. The amplifier consists of three gain stages. The first stage is core-pumped amd produces 2.7 ps pulses with 100 mW of average power. For the experiments with prechirping, a diffraction grating compressor (density of 900 line/mm and the dispersion of –0.047 ps^2/cm) is inserted after the first stage. The second stage, which delivers 5.2 ps pulses with 1 W average power, comprises a single-mode double-clad (DC) fiber pumped by a single 10 W diode. The final amplifier is composed of a multiport pump-signal combiner (MPC) with 5 pump ports, connected to a low-doped DC Yb-25/250-fiber, followed by a high-doped Yb-25/250-fiber. The low-doped segment is 1.8 m long with 6.5 dB/m absorption at 980 nm, and the high-doped segment is 1.6 m long with 10.8 dB/m absorption at 980 nm. Both fibers have the same core and clad numerical aperture, which enables very low-loss splicing between them. Apart from the hybrid doping structure, the final amplifier stage is the same as in [15], where further details can be found. We employ two 25 W diodes and three 32 W diodes, all operating at ~976 nm, for pumping. The absolute total fiber length in this system is 19.3 m, which corresponds to a total group dispersion delay (GDD) of 0.45 ps^2.

We used numerical simulations to investigate the doping management concept and to determine the optimal lengths of the fiber segments. To this end, we considered pulse formation in the oscillator, and then propagation in the optional grating compressor, the gain media, and the passive fibers. Pulse propagation is modeled using numerical simulations based on the extended nonlinear Schrödinger equation described in [16]. The group-velocity dispersion (GVD), and third-order dispersion coefficients for the fiber segments are taken as $\beta^{(2)} = 23$ fs^2/mm and $\beta^{(3)} = 43$ fs^3/mm, respectively. The parameters that describe gain, namely central wavelength, gain bandwidth, and saturation levels, were obtained from another simulation code, which implements an extended version of the three-level model described in [17]. The details of the model, utilizing wavelength-dependent emission and absorption cross-sections, are given in [18]. However, this model treats the 100 MHz pulse train as cw, which is justified given the high repetition rate. Ideally, the doping level should increase smoothly such that heat generation per unit length is kept close to, but below, a safe level. The increasing doping level along the depletion of the pump minimizes the total fiber length and more importantly the B integral. However, at present, doping levels that vary along the fiber are not available, so we focused on the use of two segments of fiber with different doping levels, spliced together. The benefits of this configuration are shown through simulation results summarized in Fig. 2. Simulations yield evolution of the signal and pump power, as well as heat generation per unit length and accumulated nonlinear phase shift for three amplifier configurations: (i) with low-doped fiber, (ii) with high-doped fiber, and (iii) with a segment of low-doped fiber, followed by a segment of high-doped fiber (i.e., implementing discrete doping management). In all cases, total gain fiber length is chosen to absorb 98% of the pump power. Prechirping is not considered, so
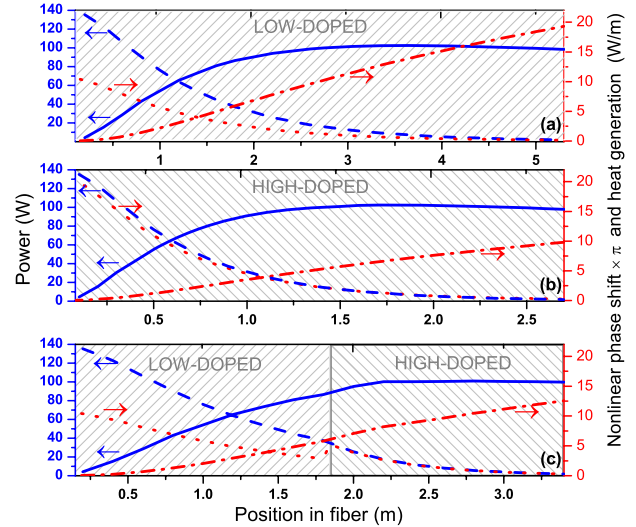

Fig. 2. (Color online) Simulated evolution of signal (solid curve) and pump (dashed curve) power, nonlinear phase shift (dot-dashed curve) and heat generation per unit length (dotted curve) along (a) low-doped, (b) high-doped, and (c) low- and high-doped, hybrid gain fibers.

the pulse duration is taken to be 13 ps. The doping concentration is taken as 5×10^{25} m^{-3} and 1×10^{26} m^{-3} for the low- and high-doped fibers, respectively. For the low-doped amplifier, the nonlinear phase shift is 19π, and the maximum heat generation is 10 W/m. For the high-doped amplifier, with its shorter length, the nonlinear phase shift is reduced to 10π, but the maximum heat generation increases to 20 W/m. For the hybrid amplifier, the maximum heat generation is the same as the low-doped fiber, at 10 W/m, whereas the nonlinear phase shift is 12.5π, representing a small increase compared to the high-doped amplifier.

Encouraged by the simulations, we have constructed the hybrid power amplifier. Figure 3(a) shows the measured power scaling behavior, in comparison to simulations using the same parameters as described above. Figure 3(b), which plots measured and simulated pulse-width versus total GDD of the system, demonstrates control of pulsewidth through prechirping. Without prechirping, the measured (simulated) pulse duration is 13 ps (12 ps). Through prechirping, the shortest pulse duration obtained experimentally is 4.5 ps, at a total GDD of –0.12 ps^2, limited by excessive nonlinear phase
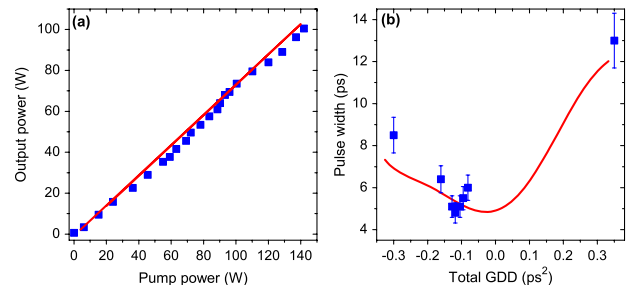

Fig. 3. (Color online) (a) Measured (squares) and simulated (solid line) output power versus pump power; (b) measured (squares) and simulated (solid line) pulsewidth at 100 W power versus total GDD of the system.
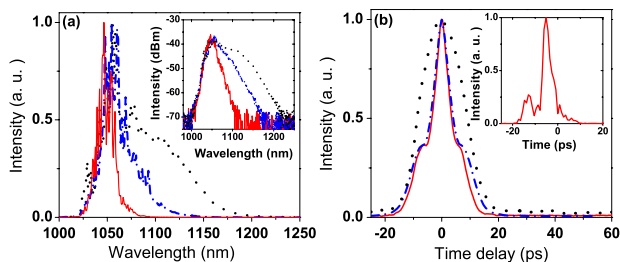
Fig. 4.   (Color online) (a) Measured optical spectra at output powers of 100 W (solid line), 70 W (dashed line), and 50 W (dotted line). Inset: semilog version of the same graph. (b) Measured intensity autocorrelation (solid curve) along with retrieved autocorrelation using PICASO (dot-dashed curve) by using grating compressor, without grating compressor (dotted curve). Inset: retrieved pulse profile.

shifts. Figure 4(a) shows the measured optical spectra at output powers of 50, 70, and 100 W. The measured intensity autocorrelation of the pulses obtained without any prechirping and the shortest pulses with prechirping are shown in Fig. 4(b). We used the PICASO algorithm to retrieve the pulse shape using measured autocorrelation and optical spectrum information [19] [Fig. 4(b)]. While PICASO-retrieval is not exact for complex pulse shapes, the retrieved pulse shape and widths are in good agreement with the simulation results.

In conclusion, we propose doping management, where the doping level of the gain fiber is varied, to mitigate the trade-off between minimizing thermal load and nonlinear processes. Ideally, one would desire a custom fiber with a varying doping level, for which our preliminary calculations indicate nearly order-of-magnitude improvements. As a first practical step, we have demonstrated a 100 W, 4.5 ps, 100 MHz amplifier using discrete doping management, which was implemented by a combination of a low-doped and a high-doped Yb fiber. Our approach can be improved upon even with existing fibers since fibers with lower and higher doping are available. In addition, for a similar effect, it may be possible to combine fibers of different core-to-cladding ratios, as long as low-loss splicing between them is possible. Consequently, we see no major impediments to the development of a four- or five-segment gain fiber, which could lead to nearly order-of-magnitude reductions in the B integral while keeping the maximum local heat generation very low. While we have focused on a picosecond amplifier in this work, doping management should equally benefit highest-power cw fiber lasers and amplifiers, since these systems are also limited by stimulated Brillouin scattering and Raman scattering [1]. Finally, the laser parameters demonstrated here with an all-fiber-integrated architecture are highly attractive for high-speed ultrafast micromachining experiments.

References

1. D. J. Richardson, J. Nilsson, and W. A. Clarkson, J. Opt. Soc. Am. B **27**, B63 (2010).
2. J. Nilsson and D. N. Payne, Science **332**, 921 (2011).
3. J. Limpert, F. Roser, D. N. Schimpf, E. Seise, T. Eidam, S. Hadrich, J. Rothhardt, C. J. Misas, and A. Tünnermann, IEEE J. Sel. Top. Quantum Electron. **15**, 159 (2009).
4. H. Kalaycıoğlu, K. Eken, and F. Ö. Ilday, Opt. Lett. **36**, 3383 (2011).
5. T. Eidam, J. Rothhardt, F. Stutzki, F. Jansen, S. Hädrich, H. Carstens, C. Jauregui, J. Limpert, and A. Tünnermann, Opt. Express **19**, 255 (2011).
6. S. P. Chen, H.-W. Chen, J. Hou, and Z.-J. Liu, Opt. Express **17**, 24008 (2009).
7. K. K. Chen, J. H. V. Price, S. Alam, J. R. Hayes, D. Lin, A. Malinowski, and D. J. Richardson, Opt. Express **18**, 14385 (2010).
8. Z. Zhao, B. M. Dunham, I. Bazarov, and F. W. Wise, Opt. Express **20**, 4850 (2012).
9. N. J. Smith, N. J. Doran, W. Forysiak, and F. M. Knox, J. Lightwave Technol. **15**, 1808 (1997).
10. F. Ö. Ilday and F. W. Wise, J. Opt. Soc. Am. B **19**, 470 (2002).
11. F. Ö. Ilday, H. Lim, J. Buckley, and F. W. Wise, Opt. Lett. **28**, 1362 (2003).
12. P. K. Mukhopadhyay, K. Özgören, I. L. Budunoğlu, and F. Ö. Ilday, IEEE J. Sel. Top. Quantum Electron. **15**, 145 (2009).
13. A. Chong, J. Buckley, W. Renninger, and F. W. Wise, Opt. Express **14**, 10095 (2006).
14. K. Özgören and F. Ö. Ilday, Opt. Lett. **35**, 1296 (2010).
15. K. Özgören, B. Öktem, S. Yılmaz, F. Ö. Ilday, and K. Eken, Opt. Express **19**, 17647 (2011).
16. B. Oktem, C. Ülgüdür, and F. Ö. Ilday, Nat. Photon. **4**, 307 (2010).
17. R. Paschotta, J. Nilsson, A. C. Tropper, and D. C. Hanna, IEEE J. Quantum Electron. **33**, 1049 (1997).
18. K. Gurel, P. Elahi, C. Senel, P. Paltani, and F. O. Ilday, in *CLEO: 2011–Laser Applications to Photonic Applications* (Optical Society of America, 2011), paper CThU5.
19. J. W. Nicholson, J. Jasapara, W. Rudolph, F. G. Omenetto, and A. J. Taylor, Opt. Lett. **24**, 1774 (1999).